Mixture Ratio and Thrust Control of a Liquid-Propellant Rocket Engine

Henrique Coxinho Tomé Raposo
henrique.raposo@ist.utl.pt

Instituto Superior Técnico, Lisboa, Portugal

November 2016

Abstract

Presently, most European launchers' engines work in open-loop. Not only does this oblige the valves which regulate the mass flow-rates to be calibrated before flight in order to obtain a desired thrust and mixture-ratio, but it also limits performance. Varying operating conditions translate into a drifting equilibrium point. The associated dispersion forces us to carry extra propellants to ensure mission success. The present work implements a closed-loop controller on the VINCI engine, aiming to maintain an optimal equilibrium point despite external perturbations, and also to transition to a 70% thrust regime. To meet these objectives, a reduced linear model of the expander thermodynamic cycle of the engine is obtained through a combination of an analytic linearization approach and a least-squares identification method. A sensitivity study confirms that 5 states suffice to describe the dominant dynamics. Two PID controllers are tuned based on the input-output pairings that minimize coupling within the 2×2 MIMO system. Modifications such as feed-forward, anti-windup and measurements filtering are made in order to match the control specifications. Simulations on the non-linear model indicate a single controller to be both capable of maintaining an operating point and of transitioning to the low-thrust regime, all while rejecting perturbations. The robustness to parameter uncertainty is assessed and preliminary results indicate actuator saturation before the controller displays any signs of instability. This work confirms the applicability of a modified PID controller to a naturally stable engine and lays the foundation to the study of other thermodynamic cycles.

Keywords: VINCI, Expander thermodynamic cycle, Thrust control, Mixture-ratio control , PID

1. Introduction

Nowadays in Europe most launchers' engines work in open-loop. As a consequence, during ground tests one needs to calibrate a number of valves in order to obtain a desired thrust and mixture ratio. They then remain with the same open-section throughout the flight. While it is true that some engines have a binary position system for the control valves which allows for some in-flight adjustment, current technology does not allow for precise control over the operating point during flight. Consequently, due to changing accelerations, overall engine ageing, and heating of the propellant tanks during the ascent, the operating point drifts during the boosted flight.

From a performance's point of view, the use of a closed loop would not only allow us to suppress certain ground tests which would no longer be necessary, but also to maintain a steady optimal operating point throughout the whole flight. Moreover, the ability to predict the engine's operating point more accurately by reducing biases and dispersions would limit the amount of extra propellants carried for security reasons, thus reducing the total mass of the launcher at take-off.

Secondly, from a reusable launching system point of view, controlling thrust and the mixture-ratio would not only allow us to limit the mechanical and thermal stresses, which would be pivotal to preserve the structure for subsequent launches, but also to take into account changing structural characteristics due to ageing. In other words, the control system should be robust to parameter uncertainties to a certain extent. Finally, landing the first stage of a launcher would undoubtedly require control over a wide range of thrust capabilities.

Partially motivated by the pressure of lower-cost competitive options in the market, there is a global European effort to enhance performances and reduce costs in the next generation of launchers, namely in Ariane 6. My thesis is inserted in this context and is intended to help the *Direction des Lanceurs* of CNES, the French Space Agency, assess the work developed by the industry on this

particular subject. It tackles three main challenges concerning the control in closed-loop of thrust and mixture-ratio of a liquid-propellant rocket engine:

1. Obtaining a low-order physical linear model of the thermodynamic cycle of the VINCI engine adapted to classical linear control techniques;
2. Analysing the dynamics of the engine to understand which of its sub-systems dominate the time-response and how their parametrization affects the dominant dynamics;
3. Implementing and validating a robust control law capable of maintaining with precision a desired equilibrium point and transitioning towards a low-thrust equilibrium point while respecting the established control requirements;

Historically, there are a number of engines which implemented throttling - a commonly used term to describe the use of valves to control propellant mass flow rates and overall thrust magnitude. Among these, the most iconic are the Lunar Module Descent Engine (LMDE), the Space Shuttle Main Engine (SSME) [2] and, more recently, SpaceX's Merlin family.

While there are several techniques to control thrust and mixture-ratio, defined as the ratio between the oxidizer and fuel's mass flow rates, throttling continues to be the simplest technique [2]. There are however limited references in the open literature on modelling and controller design for liquid-propellant rocket engines (LPRE).

Among the most relevant are [4] and [3] which describe two different linear model identification techniques for the SSME. The first uses pseudo-random binary sequences as driving signals to excite all modes of the system and a recursive maximum likelihood algorithm to determine the transfer function coefficients for a linear model around an equilibrium point. Given that the order of the system is unknown, parameters are estimated for models of increasing order until the total estimation error converges to a minimum. The second implements a least-squares technique to determine a state-space formulation of the linearized system.

In regards to the control loop, [9] discusses the implementation of an integral and proportional-integral control strategy for the Japanese LE-X cryogenic booster engine. In [1] a proportional-derivative-integral (PID) controller is tested against a fuzzy logic controller in an academic simplified model of an LPRE constituted of 1st order ordinary differential equations. Both are found to have acceptable performances although the PID displays better performance.

This extended abstract is structured in the following way: in section 2 the VINCI engine is described. In section 3 we present an overview of elements of control theory over which the present work is based. In sections 4 and 5 we describe the obtained linear models and the implementation of the control law, followed by the validation in section 6 and the conclusions in section 7.

2. VINCI Engine

In this section an overview of propulsion fundamentals is given, followed by a brief presentation of the VINCI engine, of its thermodynamic cycle, and of the control valves.

2.1. Propulsion Fundamentals

The principal function of a chemical rocket propulsion system is to generate a propulsive force - thrust - by converting chemical energy stored in the propellants into kinetic energy of the gaseous combustion products with maximum efficiency [10]. These gases are expelled at high velocities, thus creating a force given by

$$F = \dot{m} v_{\text{nozzle}} + (p_{\text{nozzle}} - p_{\text{atm}}) S_{\text{nozzle}} \qquad (1)$$

,where

- F denotes thrust, the produced force
- $\dot{m}$ is the total mass flow-rate
- v_{nozzle} is the gas velocity at the exit of the nozzle
- S_{nozzle} is the surface at the exit of the nozzle
- p_{nozzle} and p_{atm} are the atmospheric and nozzle outlet pressures

At optimal conditions, $p_{\text{nozzle}} = p_{\text{atm}}$, in which case we say the nozzle has an optimum expansion ratio, avoiding pressure losses and energy waste during the gas acceleration. Hence, if we also consider the flow through the nozzle to be isentropic, that the velocity of the flow at the combustion chamber is negligible, and that the ideal gas law applies to this component, we obtain:

$$F = S_{\text{t}} p_{\text{chmb}} \sqrt{\frac{2\kappa^2}{\kappa - 1} \left(\frac{2}{\kappa + 1}\right)^{\frac{\kappa+1}{\kappa-1}} \left[1 - \left(\frac{p_{\text{nozzle}}}{p_{\text{chmb}}}\right)^{\frac{\kappa-1}{\kappa}}\right]} \qquad (2)$$

This expression is not demonstrated here for the sake of conciseness but the proof can be found in [10]. The above result is very important because it demonstrates that thrust is only a function of the throat area S_t, the chamber pressure p_{chmb}, the specific heat ratio κ, and the pressure ratio across the nozzle $p_{\text{nozzle}}/p_{\text{chmb}}$. This means that for constant mixture ratio, and therefore constant specific heat ratio, and constant pressure ratio across the nozzle, thrust is proportional to chamber pressure. In what concerns the pressure ratio across the nozzle, at optimal conditions, it depends solely on the geometry of the nozzle itself and on the specific heat

ratio. Controlling thrust thus becomes equivalent to controlling chamber pressure.

2.2. VINCI Engine Presentation

The VINCI engine is expected to power the upper stage of the Ariane 6 launcher. Developed by Snecma, it is a liquid-bipropellant, pump-fed, expander cycle engine which uses liquid oxygen (LOX) as an oxidizer and liquid hydrogen (LH2) as a fuel, both of which are cryogenic propellants. Its characteristics at nominal level are presented in table 1 [8].

Table 1: Vinci engine nominal equilibrium point.

Vacuum thrust	180 kN
Mixture ratio	5.8
Chamber pressure	60 bar

The most detailed in-house model of this engine was built using CARINS, a code developed by CNES for rocket engine transient modelling. Much like Simulink, this software allows us to describe a system with an assemble of blocks or subsystems, each of which represents a component of the actual engine - for instance a turbo-pump or a cavity. The model is non-linear but nonetheless simplified, resorting to 0D or 1D physical models for the components.

2.3. Thermodynamic Cycle

The turbine-drive system of the VINCI engine is based on an expander cycle. Figure 1 illustrates the design. On the hydrogen side, the pump increases the pressure of the liquid fluid, which is then heated on the regenerative circuit. This element, which has an interface with the combustion chamber and the nozzle, providing the heat, is at the core of this thermodynamic cycle. The hydrogen by-pass valve (VBPH) routes a fraction of the energized mass flow to power the hydrogen turbine, in turn providing energy to the attached pump, while the rest is directly injected in the combustion chamber. Similarly, the oxygen by-pass valve (VBPO) splits the mass flow before reaching the oxygen turbine, thus providing direct control over the power transmitted to this turbo-pump. On the oxygen side the pressurized liquid oxygen is directly injected into the combustion chamber. Due to the interaction between the combustion chamber and the fuel, it is considered to be a coupled cycle. Because all of the propellants eventually reach the combustion chamber, it is also considered to be a closed cycle. While this yields maximum efficiency, it is also a limiting factor. Chamber pressure, at the downstream of the turbines, cannot surpass a certain level because a considerable pressure drop across the turbines is required to be able to generate sufficient power. Therefore, both of these quantities mutually constrain each other. Another limiting factor concerns the regenerative circuit which is the source of all power feeding the thermodynamic cycle. The limited surface area for heat exchange imposes a ceiling to the power being fed to the cycle and therefore to the generated thrust levels.

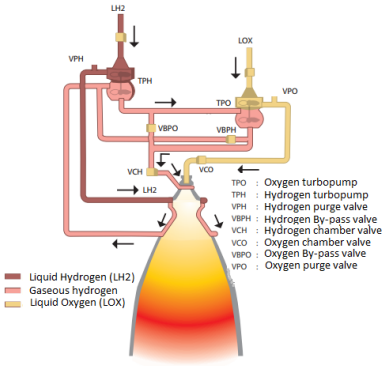

Figure 1: VINCI's synoptic [8].

2.4. Mixture Ratio and Thrust Control Organs

The VINCI engine possesses 4 valves and 4 interface parameters affecting the chamber pressure and the mixture-ratio. The VCH and VCO valves are used during the start-up and shutdown transient regimes, which fall out of the scope of this thesis. The remaining valves and interface conditions and how they affect the controlled quantities are explained below:

1. **VBPH:** this valve by-passes the flow of hydrogen to both the oxygen and the hydrogen turbo-pump systems; the chamber-pressure is the controlled quantity in this case - an increase in the open-section will decrease the mass flow rate feeding both turbo-pumps which in turn decreases the chamber pressure.
2. **VBPO:** this valve controls the relative quantity of mass flow rate passing in the oxygen and hydrogen turbo-pump systems; consequently it is able to control the relative amount of fuels being fed into the system and thus the mixture ratio;
3. **Turbo-pumps inlet conditions:** the inlet pressure and temperature of the pumps, which depend on the state of the stocked fuels, also act on the system; these four inputs are not controlled and are ideally constant for maximum performance; however, they tend to vary throughout the flight due to changing acceleration and heating of the fuel tanks; as a consequence, from a control perspective, they are considered as perturbations.

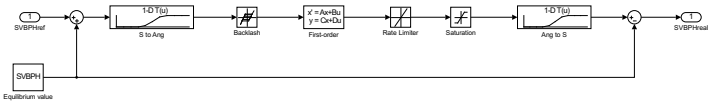

Figure 2: Valves' Simulink block diagram.

The valves work in closed-loop. For the purposes of this thesis they are modelled with a first order transfer function followed by a rate-limiter, which models the velocity saturation, a saturation, which accounts for the maximum and minimum open section of the valves, and a dead-band, which defines the accuracy. The associated Simulink model is presented in figure 2. Note that the valves are commanded in absolute geometric open angle θ. We therefore first convert the variational open hydraulic reference section into θ through an existing experimental relationship between these two quantities. The inverse of this operation is also effectuated in order to obtain the effective variational open hydraulic section.

3. Elements of Control Theory

In this section we provide an overview of the implemented techniques to obtain a reduced linear model of the VINCI engine.

3.1. State-Space Model Linearization

A system is said to be in state variable form if its dynamic model is described by n first order differential equations and p algebraic equations as follows

$$\begin{aligned} \dot{x} &= f(x_1, ..., x_n, u_1, ..., u_m) \\ y &= g(x_1, ..., x_n, u_1, ..., u_m) \end{aligned} \tag{3}$$

, where $x = [x_1, ..., x_n]^T$ is the state vector, $u = [u_1, ..., u_m]$ the control input and $[y_1, ..., y_p]$ the control output. Functions $f = [f_1, ..., f_n]^T$ and $g = [g_1, ..., g_p]^T$ are generally non-linear, as is the case of the VINCI engine. However, in order to be able to apply known linear control techniques, one can generally describe the behaviour of a non-linear system in the vicinity of a system configuration called equilibrium point by resorting to an approximate model of the form:

$$\begin{aligned} \dot{x} &= Ax + Bu \\ y &= Cx + Du \end{aligned} \tag{4}$$

Matrix A has dimensions $n \times n$, B is $n \times m$, C is $p \times n$ and D is $p \times m$.

Definition 1. *Equilibrium point* Let us consider a system in the state-space form of equation (3) and a constant input $\bar{u}$. Then if $f(\bar{x}, \bar{u}) = 0$, $\bar{x}$ is said to be an equilibrium point of the system.

The state-space form is obtained through a first-order Taylor series expansion of the dynamics about an equilibrium point, yielding

$$\begin{aligned} \Delta\dot{x} &= A\Delta x + B\Delta u \\ \Delta y &= C\Delta x + D\Delta u \end{aligned} \tag{5}$$

, where Δx denotes $x - \bar{x}$, Δu denotes $u - \bar{u}$ and Δy denotes $y - \bar{y}$. Matrices A, B, C, D are expressed as:

$$A = \left[\frac{\partial f}{\partial x}\right]_{\bar{x},\bar{u}} \qquad B = \left[\frac{\partial f}{\partial u}\right]_{\bar{x},\bar{u}}$$

$$C = \left[\frac{\partial g}{\partial x}\right]_{\bar{x},\bar{u}} \qquad D = \left[\frac{\partial g}{\partial u}\right]_{\bar{x},\bar{u}}$$

It is worth mentioning that the linearization is only valid in a sufficiently small domain around the equilibrium point, the extent of which depends on the particular application at hand and may be difficult to compute.

3.2. Matched DC Gain Reduction Method

The process of obtaining a low-order model from a high-order complete model is commonly called model order reduction. A possible technique is to use physical insight to remove model states while preserving the input-output behaviour of a system, particularly at low frequencies. Let us consider the classical state-space model formulation of equation (4). The state-vector x can be decomposed as $x = [x_{nr}, x_r]^T$, where x_{nr} constitutes the set of states to be kept and x_r the set of states to be eliminated. The state-space model thus becomes:

$$\begin{aligned} \begin{bmatrix} \dot{x_{nr}} \\ x_r \end{bmatrix} &= \begin{bmatrix} A_{11} & A_{12} \\ A_{21} & A_{22} \end{bmatrix} \begin{bmatrix} x_{nr} \\ x_r \end{bmatrix} + \begin{bmatrix} B_1 \\ B_2 \end{bmatrix} u \\ y &= \begin{bmatrix} C_{11} & C_{12} \\ C_{21} & C_{22} \end{bmatrix} \begin{bmatrix} x_{nr} \\ x_r \end{bmatrix} + \begin{bmatrix} D_1 \\ D_2 \end{bmatrix} u \end{aligned} \tag{6}$$

Assuming the dynamics of x_r to be infinitely fast, then $\dot{x}_r \approx 0$ and the model can be rewritten as:

$$\dot{x}_{nr} = (A_{11} - A_{12}A_{22}^{-1}A_{21})x_{nr} + (B_1 - A_{12}A_{22}^{-1}B_2)u \tag{7}$$

$$y = \begin{bmatrix} (C_{11} - C_{12}A_{22}^{-1}A_{21}) \\ (C_{21} - C_{22}A_{22}^{-1}A_{21}) \end{bmatrix} x_{nr} + \begin{bmatrix} (D_1 - C_{12}A_{22}^{-1}B_2) \\ (D_2 - C_{22}A_{22}^{-1}B_2) \end{bmatrix} u \tag{8}$$

The matched DC-gain method preserves the static gain of the original full model. Moreover, when compared to other more sophisticated methods, this has the advantage of conserving the state-space base, in other words, the reduced model can be interpreted physically if the full model has an explicit physical-related state-vector. This is of first

importance to our objectives because it will allow us to determine which elements and physical parameters within the engine play a significant role in the system's dominant dynamics.

One of its main disadvantages, however, concerns the choice of the set of states to be eliminated. That analysis has to be made on a model to model basis and is often based on physical insight of the dynamics of the system.

3.3. Least-Squares Identification Method

Often, in the world of physics we expect to find linear relationships between variables. Seldom, however, are these relations perfectly linear due to experimental errors and, frequently, to approximately linear phenomenons. Nonetheless, in order to simplify our models, we look to establish "the best" linear fit to the observed data [6]. Let us consider the example of a discrete state-space linear model given by

$$\begin{array}{ll} x_{k+1} & = Ax_k + Bu_k \\ y_k & = Cx_k + Du_k \end{array} \tag{9}$$

This model can be rearranged as

$$\left[\begin{array}{cc} x_{k+1}^T & y_k^T \end{array}\right] = \left[\begin{array}{cc} x_k^T & u_k^T \end{array}\right] \left[\begin{array}{cc} A^T & C^T \\ B^T & D^T \end{array}\right]$$

for $k = 1, ...N$. In matrix form, this yields

$$Y = \Theta M \Leftrightarrow \left[\begin{array}{cc} x_2^T & y_1^T \\ \vdots & \vdots \\ x_{N+1}^T & y_N^T \end{array}\right] = \left[\begin{array}{cc} x_1^T & u_1^T \\ \vdots & \vdots \\ x_N^T & u_N^T \end{array}\right] \left[\begin{array}{cc} A^T & C^T \\ B^T & D^T \end{array}\right]$$

, which for N greater than the number of states of the system becomes an overdetermined system. The least-squares approach [5] consists of finding the solution which minimizes the following error function:

$$E = \| \Theta M - Y \|^2 \tag{10}$$

Calculating the gradient of this function and imposing $\frac{\partial E}{\partial M} = 0$ to obtain the minima gives

$$M = (\Theta^T \Theta)^{-1} \Theta^T Y \tag{11}$$

,which corresponds to the pseudo-inverse of matrix Θ multiplied by Y.

This method is often inadequate for model identification because it requires knowing both the order and the states of the system. On the other hand, when this is known, it has the advantage of yielding a model with the desired state-space base. In order to completely capture the system's dynamics the sampling frequency must respect Shannon's theorem which states that it ought to be at least twice as large as the natural frequency of the fastest mode.

4. Low-order Physical Linear Model

In this section we present the obtained analytic and identified linear models based on the techniques described in section 3. The nominal equilibrium point was characterized in table 1.

4.1. Analytical Model

A priori, the VINCI engine is known to be a 2×2 MIMO system, with the chamber pressure and mixture ratio as controlled outputs and the two valves' sections as controlled inputs. Our approach to obtain an analytic linear model consists of linearizing the governing equations for each of the elements that compose the engine around a generic operating point - for instance the pump, the turbine and the combustion chamber. Because we don't have access to an explicit non-linear state-space formulation, it is not possible to simply calculate the gradients at the equilibrium point. Nor is it possible, for that matter, to perform a numerical linearization of the non-linear model in CARINS.

Hereafter we present the short list of simplifications and assumptions that were made:

1. We reduce the number of elements modelling the engine when compared to the original model;
2. The ideal gas law is used instead of the real gas tables;
3. Density is supposed constant in liquid state.

Hereafter, only the linearization of the governing equations of the adiabatic pipes are presented and discussed, as an example (model extracted from CNES internal documentation). The non-linear model is given by

$$\textit{where} \quad \frac{dq}{dt} = \frac{S}{L}(p_e - p_s - \frac{k_p + 1}{2\rho_e S^2} q^2) \tag{12}$$

- q is the mass flow-rate;
- S is the surface section, with an associated diameter which is considered to be much lower than length;
- L is the length of the pipe;
- p_e and p_s are the inlet and outlet pressures, respectively;
- k_p is the pressure loss coefficient;
- ρ_e is the inlet density;

The flow is supposed to be incompressible, adiabatic and isothermal. Both density and temperature are considered to be constant. After linearization one obtains

$$\frac{d\delta q}{dt} = -\frac{(k_p+1)q_0}{LS\rho_{e_0}}\delta q - \frac{S}{L}\delta p_s + \frac{S}{L}\delta p_e + \frac{(k_p+1)q_0^2}{2SL\rho_{e_0}^2}\delta\rho_e \tag{13}$$

where the subscript 0 indicates a steady-state quantity. In the case of an adiabatic pipe, no further simplifications are required because the linear first-order differential equation is already only a function of state variables. Both pressure and density at the inlet and outlet are state variables of the cavity's model, which is the component the pipes are connected to.

In general, though, there is an extra step where we omit every intermediary variable which is not a state. For example, a cavity is described by two first-order differential equations in terms of density and pressure. Its temperature, on the other hand, is computed using the ideal gas law and might be an intervening variable in subsequent elements. Therefore, we seek to rewrite temperature as a function of density and pressure which in turn are state-space variables. These simplifications allow us to obtain a classical $\dot{x} = Ax + Bu$ form. For the sake of conciseness these calculations are not presented here. The pressure and temperature at the inlet of the pumps are included as inputs. Consequently we obtain a 6 inputs (2 controlled, 4 perturbations), 39 states and 2 controlled outputs system.

The comparison between the time-response of the full analytic linear model and the non-linear model is presented in figure 3. There is a clear mismatch of static gains, particularly on the VBPH to chamber pressure transfer function. The unsteady time-response, on the other hand, presents the same shape, notably the non-minimum phase behaviour of the chamber pressure. Due to several simplifications and hypothesis that were made while developing this model, as well as to the extent and complexity of the calculations, a fitting linear model could not be found. Let us consider that it is nonetheless representative of the behaviour of a liquid-propellant rocket engine with an expander cycle. Under this assumption, we seek to obtain a low-order linear-model that models the dominant dynamics of the engine with the method described in section 3.2. After a series of trial and error essays along with the feedback from the propulsion experts we found the five states which dominate the dynamic response of the system. They are the rotational speeds of both turbines, an hydrogen thermodynamic property at the inlet of the regenerative circuit, an hydrogen thermodynamic property at the cavity with the biggest volume, and the temperature of the wall modelling the interface of the regenerative circuit.

The time-response of the reduced model is also plotted in figure 3. It is highly representative of the

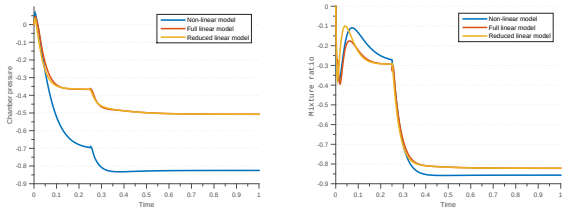

(a) Chamber pressure (b) Mixture ratio

Figure 3: Linear and non-linear models time-response comparison to a VBPH and VBPO section steps of 1% of the nominal value.

dominant dynamics of the engine, failing only to describe with high accuracy the unsteady behaviour of the mixture ratio when the VBPH is excited. This was found to be linked to the absence of the dynamics of the flow on the remaining cavities which were all considered to be instantaneous.

4.2. Identified Model

We tested the above conclusions by identifying a reduced linear model with the same five states using the least-squares identification method presented in section 3.3. A 39 states model was also identified in order to validate the algorithm. The system was excited with section steps of 1% of the nominal values for both the VBPH and the VBPO. The sampling frequency is 200Hz. The time-responses are presented in figure 4.

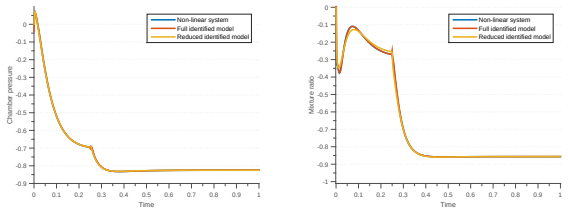

(a) Chamber pressure (b) Mixture ratio

Figure 4: Linear and non-linear models time-response comparison to a VBPH and VBPO section steps of 1% of the nominal value.

It is observed that the reduced linear model is almost a perfect fit, the representation error being again higher in the VBPH to chamber pressure transfer function, which is coherent with what was seen for the analytic model. Therefore, we are able to conclude that these five states are sufficient to describe the dominant dynamics of the VINCI engine.

The poles of the model are presented in table 2, adimensionalized by the lowest frequency pole. The settling-times of the time-response are not dominated by the slowest pole of the system. What we observe is closer to the settling time of a second order system with a pair of complex conjugate

Table 2: Poles of the reduced identified linear model.

Pole	Damping	Frequency
-1	1	1
-2.41±0.24i	0.995	2.41
-6.95	1	6.95
-60.21	1	60.21

poles such as the ones of the reduced identified linear model. This can be explained by the presence of a zero in the vicinity of the slowest pole which partially cancels its dynamic response.

The non-minimum phase behaviour can be physically explained by a sudden increase of hydrogen mass-flow rate exiting the hydrogen pump to match what is imposed by the valve. This is accompanied by a pressure drop on all cavities between the inlet of the regenerative circuit and the valve, though the output pressure of the pump remains constant because the turbine has not yet had the time to lower its regime. This phenomena accounts for an increase in mass flow rate which also explains the initial decrease in mixture ratio. The following oscillations of mixture ratio occur due to a difference of response time between the hydrogen and the oxygen turbo-pumps.

The validity of the linear model decreases when the engine's regime drifts away from the nominal equilibrium point. At 130kN of thrust, a decrease of approximately 28%, the static gains of a small perturbations model decrease significantly, as presented in table 3.

Table 3: Static gain reduction of the 130kN linear model compared to the 180kN linear model.

	VBPH	VBPO
PCC	-19%	-47%
MR	-25%	-54%

Lastly, in order to understand the association between the modes and the sub-components of the engine we performed a sensitivity analysis to the moments of inertia of the turbo-pumps, the heat capacity of the surface exchange of the regenerative circuit, and the volume of the biggest hydrogen cavity and of the regenerative circuit inlet cavity, all of which do not affect the static gain of the system. Only the time-responses for the first parameter are presented in figure 5.

The following conclusions were drawn:

1. The slowest pole is associated with the interface wall dynamics along with its near zero, having little effect on the time-response;
2. The turbo-pump systems are associated with the dominant complex conjugate pair of poles, which significantly affect the settling-times;
3. The volume of the biggest hydrogen cavity plays a major role in the transient time-response of the VBPH to mixture ratio transfer function by lagging the time-response of the hydrogen mass flow rate arriving at the inlet of the combustion chamber;
4. The cavity at the inlet of the regenerative circuit was found to model the non-minimum phase behaviour which is coherent with the previously proposed explanation of this phenomenon;

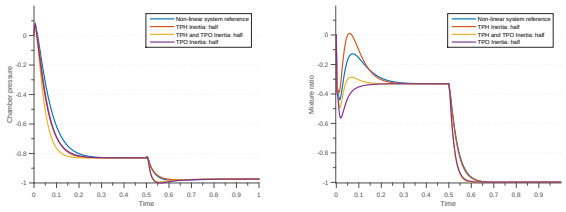

(a) Chamber pressure (b) Mixture ratio

Figure 5: Step time-responses for varying moments of inertia of the turbo-pumps.

5. Control Law Design

In this section we describe the design of a PID control law and we present the simulation results on the linear model. The relative gain array $R(0)$ [7] is a useful tool in determining the best input-output pairing for decentralized control of a multi-variable system.

$$R(0) = \begin{bmatrix} 1.09 & -0.09 \\ -0.09 & 1.09 \end{bmatrix} \tag{14}$$

The larger positive values on the diagonal indicate that we should pair VBPH - chamber pressure and VBPO - mixture ratio in order to minimize interactions between the crossed inputs-outputs. Upon designing and tuning a PID controller for each of these pairings, taking into account the model of the valves described in section 2, we obtain the variational time-responses shown in figure 6. We present both the simulation results for ideal sensors and for sensors modelled using a Gaussian additive noise centred at zero as well as a time-delay. This test-case is representative of the corrections to be made during stabilised flight when we will seek to maintain thrust while regulating the mixture ratio to optimize the consumption of the propellants.

The PID controllers were tuned with SISO tools from MATLAB. Several improvements were added:

1. A feed-forward solution in order to accelerate the time-response and decrease coupling while maintaining stability was adopted.

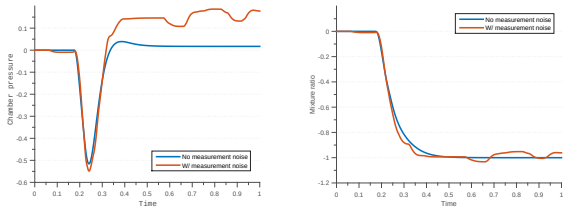

(a) Chamber pressure (b) Mixture ratio

Figure 6: Output time response to a step of mixture ratio MR $= -1$ on the complete linear model.

2. In order to prevent violent responses from the engine, the reference signals undergo a pre-treatment, eliminating any residual overshoots. The cut-off frequency of the low-pass filter approximately equals that of the slowest pole of the system.
3. Second order filters were used to treat the chamber pressure and mixture ratio measurements. It is worth noting that the latter is a pseudo-sensor because no such sensor will be available during flight. Instead, an estimator will be implemented. For the purposes of our study we consider an equivalent sensor.

The controller works at a high enough frequency not to deteriorate the time-responses of the closed-loop system. Let us also note that the tuning of the controller is coupled with the dynamics of the actuators which are not fast enough to be neglected.

Figure 7 presents the block diagram architecture. The controller block contains both the PID's and the feed-forward.

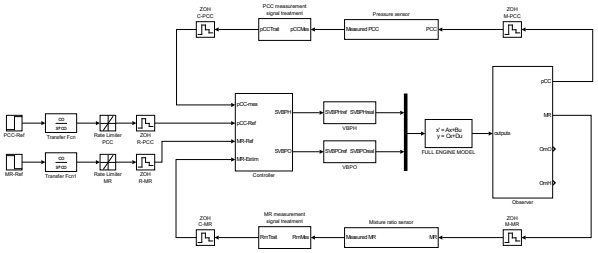

Figure 7: Closed-loop block diagram.

The time-response satisfies the unsteady and steady-state time-response specifications (in adimensional units with respect to figure 6):

1. Overshoot: less than 3 pressure units of chamber pressure and 0.5 of mixture ratio;
2. 95% settling-time: in-between 1/6 and 1/3 time units;
3. Required precision: ± 0.6 of chamber pressure and ± 0.2 of mixture ratio.

Moreover the closed-loop presents a modulus margin of 0.73, above the 0.5 reference from the literature [7], which is absolutely essential to cope with model uncertainty. Robustness will be further discussed in the next section.

6. Results

The purpose of this section is to validate the implemented control law and present the results of a simplified flight simulation.

6.1. Simplified Flight Simulation

In order to validate the control law we start by performing a simplified flight simulation on the non-linear CARINS model. We introduce input perturbations that increase linearly with time at the inlet temperature and pressure of both pumps. These are representative of the changing inlet conditions during flight due to the heating of the tanks. The engine ageing is modelled through a changing thermal flux between the combustion chamber and the regenerative circuit. A degradation of the hot wall surface between these two components is taken into account by a linearly increasing section. Other parameters assume their nominal values.

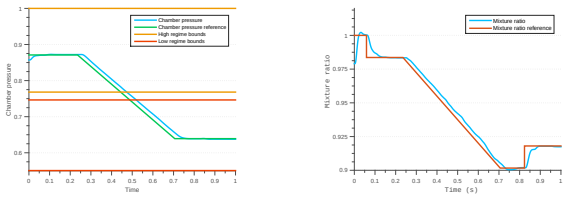

(a) Chamber pressure (b) Mixture ratio

Figure 8: Non-linear system flight simulation results.

As previously, we introduced small mixture-ratio step-like corrections. Moreover, there is a regime transition lasting 0.47 times units which lowers thrust from 180kN to 130kN. The results in figure 8 confirm the robustness of the controller on the nominal engine to a changing equilibrium point, to the non-linearities present in the CARINS model and to a more realistic high frequency model of the engine. Stability and performance remain within the specifications. The mechanical and thermal bounds of the sub-systems of the engine were also confirmed to remain within the specifications.

6.2. Robustness Analysis

It is highly important to ensure that the tuned control law is robust to model uncertainty, including parametric uncertainty and neglected or unmodelled dynamics. The former is undoubtedly relevant to our analysis mainly due to component ageing throughout the flight, manufacturing tolerances or physical characteristics of the subsystems which are not known with a high degree of precision. The

latter may include non-linearities that evidently are not represented in the linearized model, unmodelled high frequencies due to the limited scope of the identification method and changing operating conditions such as when we will transition from the 180kN to the 130kN equilibrium point.

Our validation of the control law was made in two steps. On the complete linear model we simulated flight conditions over a finite set of engine models with varying parameters and operating conditions. Both the stability and the performance were evaluated over the uncertainty set. They were evaluated through the indicators below:

1. Modulus margin;
2. Chamber pressure and mixture ratio overshoot during the equilibrium point transition.
3. Maximum difference between the chamber pressure and the chamber pressure reference during the 180kN and 130kN stabilized regimes; Idem for the mixture ratio.
4. Chamber pressure and mixture ratio 95% settling times;

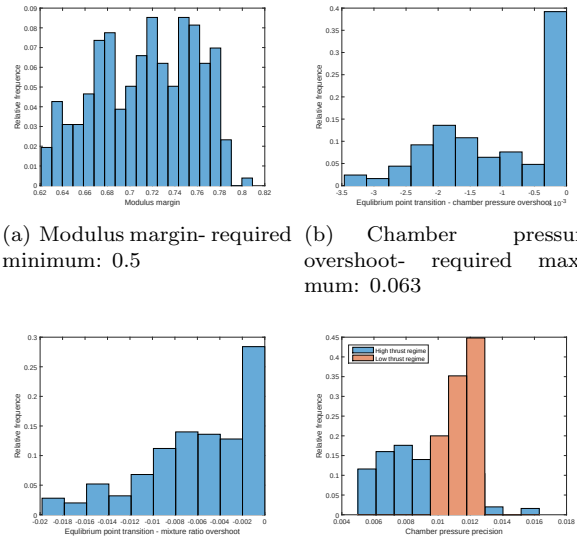

(a) Modulus margin- required minimum: 0.5

(b) Chamber pressure overshoot- required maximum: 0.063

(c) Mixture ratio overshoot- required maximum: 0.083

(d) Chamber pressure precision- required maximum: 0.013

Figure 9: Relative frequency histograms of the performance parameters.

On the non-linear model, we simulate a limited number of the worst cases in terms of stability and performance found during the linear analysis.

The chamber pressure and mixture ratio reference values follow the same profile of figure 8, without the last mixture ratio correction which in the linear model is equivalent to the first one.

The parameters which were found to have a sizeable effect over the dynamics of the engine include the moments of inertia of the turbo-pumps (J), the section of the heat exchange wall of the regenerative circuit S_{ch}, the characteristic curves of the hydrogen pump and turbine and the efficiency of the hydrogen pump (η_H). The hydrogen turbine efficiency is taken into account in its characteristic. The uncertainty over the characteristic curves is modelled through scaling multiplicative factors EPH, CPH, ETH and CTH respectively.

The uncertainty set includes all of the possible combinations of the extremes of the domains. Its main disadvantage is that it does not strictly assure us to capture the worst possible configuration for these particular domain variations. For each model of a total of 256 (2^8) of the uncertainty set, a corresponding linear model is obtained with the identification technique presented in section 3.3. The results of the simulations, under the form of histograms, are presented in figures 9 and 10.

Firstly, let us note that for a total of 28 models the engine is not capable of reaching either the 130kN or the 180kN regimes. The root cause is the saturation of the valves which render it impossible to attain these equilibrium points. It should be highlighted that these points could not have been reached in open-loop either. Saturation was thus disregarded, without compromising the conclusions about robust stability. Both because the project is still at an early phase and because we lack definitive data about the uncertainties, we refrain from trying to quantify the probability of having said cases.

Apart from the chamber pressure precision which, for a handful of cases, trespasses the threshold, all performance and stability requirements are met.

In the non-linear model we have chosen to run the flight simulation for the engines which yielded the lowest modulus margin and the highest overshoot in chamber pressure and mixture ratio. The flight simulation results are presented in figure 11. It was observed that for two out of the three simulations there were saturations of the valves. Consequently, we implemented an anti-windup to prevent the integral term of the PID controller from growing indefinitely when the valves are saturated, thus enhancing the time-response after desaturation.

It is clear that the engine is not dimensioned to handle these extreme dispersions of the selected parameters, either indicating that the parameter uncertainties were over-dimensioned or that the engine design must be re-evaluated. Performance evaluation in the case of saturation is thus meaningless. Until further information is made available we can only conclude from this preliminary robustness assessment that the closed-loop remains stable in all cases despite intrinsic performance limitations of the engine.

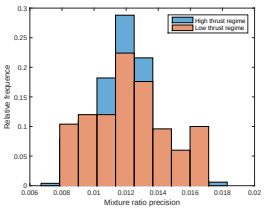

(a) Mixture ratio precision- required maximum: 0.033

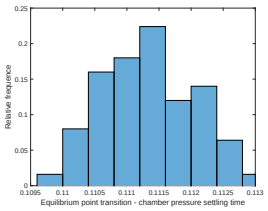

(b) Chamber pressure settling time- reference value: 0.1096

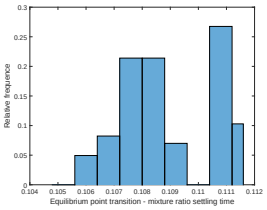

(c) Mixture ratio settling time- reference value: 0.1096

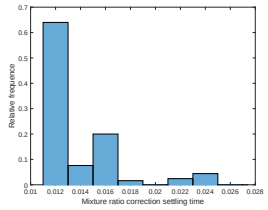

(d) Mixture ratio correction settling time- required maximum: 0.028

Figure 10: Relative frequency histograms of the performance parameters.

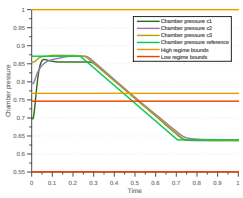

(a) Chamber pressure

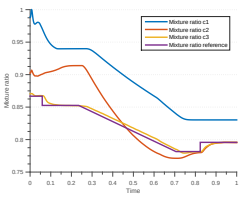

(b) Mixture ratio

Figure 11: Non-linear system flight simulation results for the worst-cases.

7. Conclusions

Motivated mainly by the necessity of improving the performances of current European launchers, a methodology to model the dynamics of a rocket engine and to design a control law was established.

An analytic approach to obtain a small perturbations model was employed. In the face of poor model accuracy, a least-squares identification method was proposed to validate the model reduction and to obtain a highly accurate low-order model. One of the main achievements is the understanding of the dominant dynamics of an expander cycle rocket engine. The implementation of a double PID controller with improvements such as feedforward, anti-windup, measurements treatment and setpoint reference signal treatment, demonstrated the applicability of this controller to a stable engine such as the VINCI. While a more rigorous robustness analysis is needed as soon as more information about the engine is made available, it was still observed that the engine will sooner saturate due to its own design than the control law will render the system unstable.

There are several subjects of the developed work that warrant further research. Firstly, the analytic approach to obtain a linear-model should be employed in a different engine in order to better comprehend the reasons for its misrepresentation. The engine analysis, which was effectuated solely for five different parameters, could be extended to other parameters of interest. The application of the same methodology to other engines with different thermodynamic cycles should be considered. In view of the difficulty of the control problem, new approaches to design the controller may be put in place, for instance structured H-infinity coupled with a PID. In order to fully validate the control law it is also necessary to design a mixture-ratio estimator and evaluate its impact on the overall performance and stability of the closed-loop system.

References

[1] A. Allahverdizadeh and B. Dadashzadeh. A fuzzy logic controller for thrust level control of liquid propellant engines. *Scientific Cooperations International Workshops on Electrical and Computer Engineering Subfields*, 2014.

[2] M. J. Casiano, J. R. Hulka, and V. Yang. Liquid-propellant rocket engine throttling: A comprehensive review. *Journal of Propulsion and Power*, 2010.

[3] A. Duyar, V. Eldem, W. C. Merril, and T. Guo. Space shuttle main engine model identification. *Journal of Dynamic Systems, Measurement, and Control*, 1989.

[4] A. Duyar and T. Guo. Space shuttle main engine model identification. *IEEE Control Systems Magazine*, 1990.

[5] C. L. Lawson and R. J. Hanson. *Solving Least squares problems*. Society for Industrial and Applied Mathematics, 1987.

[6] S. J. Miller. The method of least squares. *Mathematics Department Brown University*, pages 1–7, 2006.

[7] S. Skogestad and I. Postlethwaite. *Multivariable Feedback Control: Analysis and Design*, chapter 2-4,7,Appendix A. John Wiley and Sons, 2005.

[8] Snecma. Propulsion spatiale - vinci, 2011. Retrieved from: http://www.safran-aircraft-engines.com/fr/file/download/fiche_vinci_2011_hd.pdf.

[9] H. Sunakawa, A. Kurosu, K. Okita, W. Sakai, S. Maeda, and A. Ogawara. Automatic thrust and mixture ratio control of the LE-X. *44th AIAA/ASME/SAE/ASEE Joint Propulsion Conference and Exhibit*, 2008.

[10] G. P. Sutton and O. Biblarz. *Rocket Propulsion Elements*, chapter 2-4. John Wiley and Sons, 2001.